

TaS_2-based saturable absorbers for *Q*-switched fiber laser applications

Qinghua Wang(汪情华), Hao Sun(孙昊), Chenhao Lu(鲁晨浩), Huiran Yang(杨慧苒), and Lu Li(李璐)
Citation: Chin. Phys. B, 2025, 34 (**7**): 074209. DOI: 10.1088/1674-1056/addcd7
http://cpb.iphy.ac.cn; http://iopscience.iop.org/cpb

What follows is a list of articles you may be interested in

Broadband third-order optical nonlinearities of layered franckeite towards mid-infrared regime

Zhi-Qiang Xu(徐志强), Tian-Tian Zhou(周甜甜), Jie Li(李洁), Dong-Yang Liu(刘东阳), Yuan He(何源), Ning Li(李宁), Xiao Liu(刘潇), Li-Li Miao(缪丽丽), Chu-Jun Zhao(赵楚军), and Shuang-Chun Wen(文双春)
Chin. Phys. B, 2024, 33 (**10**): 104208. DOI: 10.1088/1674-1056/ad6ccb

Continuous wave and active *Q*-switched operation of Watt-level LED-pumped two-rod Nd,Ce:YAG laser

Jian-Ping Shen(沈建平), Peng Lu(芦鹏), Shao-Cong Xu(徐少聪), Rong-Rong Jiang(江容容), Yang Chen(陈阳), Liang Chen(陈亮), and Feng-Yang Xing(邢凤阳)
Chin. Phys. B, 2024, 33 (**7**): 074207. DOI: 10.1088/1674-1056/ad34c9

Single-frequency linearly polarized *Q*-switched fiber laser based on Nb_2GeTe_4 saturable absorber

Si-Yu Chen(陈思雨), Hai-Qin Deng(邓海芹), Wan-Ru Zhang(张万儒), Yong-Ping Dai(戴永平), Tao Wang(王涛), Qiang Yu(俞强), Can Li(李灿), Man Jiang(姜曼), Rong-Tao Su(粟荣涛), Jian Wu(吴坚), and Pu Zhou(周朴)
Chin. Phys. B, 2023, 32 (**7**): 074203. DOI: 10.1088/1674-1056/acad6d

Antimonene-based saturable absorber for a soliton mode-locked and *Q*-switched fiber laser in the 2 μm wavelength region

H Ahmad, B Nizamani, M Z Samion, N Yusoff, and M F Ismail
Chin. Phys. B, 2023, 32 (**6**): 064205. DOI: 10.1088/1674-1056/ac891f

Mid-infrared lightly Er^{3+}-doped CaF^2 laser under acousto-optical modulation

Yuan-Hao Zhao(赵元昊), Meng-Yu Zong(宗梦雨), Jia-Hao Dong(董佳昊), Zhen Zhang(张振), Jing-Jing Liu(刘晶晶), Jie Liu(刘杰), and Liang-Bi Su(苏良碧)
Chin. Phys. B, 2023, 32 (**3**): 034203. DOI: 10.1088/1674-1056/aca4c0

TaS_2-based saturable absorbers for Q-switched fiber laser applications

Qinghua Wang(汪情华)[1], Hao Sun(孙昊)[1,2,3,†], Chenhao Lu(鲁晨浩)[4], Huiran Yang(杨慧苒)[4], and Lu Li(李璐)[4,‡]

[1] *School of Material Science and Engineering, Inner Mongolia University of Science and Technology, Baotou* 014010, *China*
[2] *Inner Mongolia Key Laboratory of New Metal Material, Baotou* 014010, *China*
[3] *Key Laboratory of Green Extraction & Efficient Utilization of Light Rare-Earth Resources, Ministry of Education, Baotou* 014010, *China*
[4] *School of Science, Xi'an University of Posts and Telecommunications, Xi'an* 710121, *China*

(Received 21 April 2025; revised manuscript received 7 May 2025; accepted manuscript online 26 May 2025)

Transition metal disulfides are widely applied as nonlinear optical materials for laser pulse generation. In this paper, TaS_2 is successfully used for the first time to achieve a high-energy passively Q-switched erbium-doped fiber (EDF) laser. TaS_2 nanosheets are prepared by the liquid phase exfoliation method, and then the TaS_2 solution is mixed with polyvinyl alcohol (PVA). TaS_2/PVA film is prepared, which is cut into 1 mm × 1 mm flakes. TaS_2/PVA saturable absorber (SA) is obtained by sandwiching a small flake between two fiber optic patch cable connectors. With the TaS_2/PVA SA added to an EDF laser, a Q-switched fiber laser with a center wavelength of 1560 nm and a repetition rate ranging from 51.33 kHz to 83.04 kHz is realized. At the pump power of 231 mW, the maximum output power is 1094 μW, and the shortest pulse duration is 3.48 μs. The results confirm that the TaS_2 material has excellent potential for application in nonlinear optics.

Keywords: transition metal disulfide, Q-switched, saturable absorber, fiber laser

PACS: 42.55.Wd, 42.70.Gi, 42.70.–a

DOI: 10.1088/1674-1056/addcd7 **CSTR:** 32038.14.CPB.addcd7

1. Introduction

The Q-switched fiber laser has the advantages of high-power pulse output, compactness, lightweight, high efficiency, wavelength tunability, stability and reliability, and ease of control. These merits have led to a growing demand for more efficient and cost-effective Q-switched lasers. For example, pulse lasers have been used in some laser surgeries and laser therapies in the medical field.[1,2] High peak power pulse lasers can be used for metal cutting and drilling in industrial processing.[3–5] Beyond these applications, Q-switched lasers are also widely employed in fiber-optic communications, optical data storage systems, and lidar (laser radar) technologies.[6–11] Passive Q-switched lasers have been more desirable than their active counterparts because they are structurally simple, and have stable output power and high output beam quality.[12–16]

Generally, to achieve passive Q-switched operation, an optical modulator is usually required to modulate the quality factor.[17] A saturable absorber (SA) is an excellent quality modulator for generating uniform pulses in Q-switched fiber lasers,[18–23] which enables the energy storage-release cycle in Q-switched fiber lasers through dynamic intra-cavity loss modulation and nonlinear absorption shaping. For decades, semiconductor saturable absorber mirrors (SESAMs) have been considered among the best and most cost-effective SA options.[24] However, SESAMs suffer from a narrow absorption wavelength range, which limits their performance. Therefore, the continuous search for low-cost, large-bandwidth, and high-performance SAs remains an ongoing problem. In a previous study, nanomaterial-based SAs, such as carbon nanotubes (CNTs), graphene, topological insulators (TIs), transition metal dichalcogenides (TMDs), and black phosphorus (BP) have attracted researchers' attention, and have been extensively studied and proven to be important substitutes for SAs in pulsed laser setups for generating ultrashort pulses.[25–30] The generic term TMD refers to the combination of sulfur atoms (S, Se, and Te) with transition metals (groups IVB to VIII, IB, and IIB). In fact, VIB group TMDs (MoS_2 and WS_2) have been extensively employed for pulse creation.[31,32] In addition, some other TMDs with small band gaps, including ReS_2 and HfS_2, have also been used as SAs.[33,34] However, ultrafast photonic devices based on VB TMDs are still in the early stages of development. TaS_2 is a representative of conducting VB TMDs, consisting of metallic tantalum in the form of S–Ta–S sandwiched between two sulfide layers with negligible band gap metal behavior. TaS_2 can be used in energy technology, photovoltaic devices, electrochemical energy storage, and other multifunctional application areas where it offers outstanding advantages.[35–38]

In this work, we demonstrate the successful application of TaS_2/polyvinyl alcohol (PVA) as an SA in a Q-switched

†Corresponding author. E-mail: sunhao2580@163.com
‡Corresponding author. E-mail: liluyoudian@xupt.edu.cn

© 2025 Chinese Physical Society and IOP Publishing Ltd. All rights, including for text and data mining, AI training, and similar technologies, are reserved.

erbium-doped fiber (EDF) laser. The SA thin film has the advantages of a simple preparation process, good homogeneity, and flexibility. Stable Q-switched pulses are achieved by integrating the TaS_2/PVA SA into the EDF laser cavity. The laser generates uniform Q-switched pulses centered at 1560 nm. As the pump power increases from 118 mW to 231 mW, the repetition rate rises nearly linearly from 51.33 kHz to 83.04 kHz, while the pulse duration decreases from 6.5 μs to 3.48 μs. The Q-switched fiber laser operates in a saturated state without damaging TaS_2/PVA SA. The experimental results indicate that TaS_2 can be used as a Q-switched device for generating ultrashort pulses. Furthermore, it promotes the advancement of ultrafast optical devices based on two-dimensional (2D) materials.

2. Fabrication and characterization of TaS_2 nanosheets

In this paper, the TaS_2/PVA SA was prepared by the liquid phase exfoliation method. Isopropyl alcohol (IPA) is a commonly used solvent with excellent solubility. As a solvent, it is widely used as an economical and practical solvent in industry, which can be mixed freely with water, and has stronger solubility than ethanol for lipophilic substances. Some 2D nanomaterials disperse well in IPA. Therefore, in this work, IPA was chosen as the solvent to prepare the TaS_2/PVA SA. 6 mL deionized water was added to 0.45 g PVA powder and sonicated uniformly. Then, 11 mg TaS_2 powder was dispersed into 6 mL IPA, and ultrasonically cleaned for 10 h. The ultrasonic cleaner's power was set to 150 W. Finally, PVA and TaS_2 IPA solutions were mixed at a 1:2 ratio, yielding the mixture shown in Fig. 1(a).

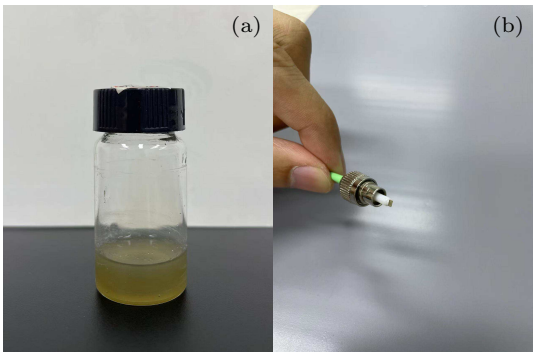


Fig. 1. (a) The photograph of TaS_2 nanosheets dispersion. (b) Glue TaS_2/PVA SA to the end of the optical fiber connector.

The obtained mixture solution was shaken well and decanted into the plastic vessels. Subsequently, the plastic vessels were put into the drying oven, and the temperature of the drying machine was set at 50–55 °C. The time required for the TaS_2/PVA SA to dry was about two days. After drying was completed, the film was adhered to the inner walls and bottom of the plastic vessel. The PVA solution exhibits strong wet adhesion to plastic surfaces, enabling uniform coating of container walls. Upon drying, the PVA film lost interfacial adhesion, allowing for facile peeling from the plastic substrate. The TaS_2/PVA film on the wall of the container was used as the SA, because it has higher quality than that on the bottom. The TaS_2 film was cut into small pieces of 1 mm×1 mm and adhered to the end of the fiber optic connector, as shown in Fig. 1(b).

For more detailed material characterization, the solution was deposited onto a silicon substrate, which minimally affects the measurements. A Raman spectrometer with an excitation wavelength of 532 nm was used to analyze the vibration modes of TaS_2. The measurement results are shown in Fig. 2(a). We can see four peaks with different vibrational modes. The sweep range is set from 0 to 700 cm^{-1}, and the out-of-plane mode of TaS_2 vibration includes the A_{1g} peak observed at 400.31 cm^{-1}. The E_{1g} peak at 109.85 cm^{-1} and E^1_{2g} peak at 288.73 cm^{-1} reflect the in-plane mode of vibration of TaS_2. The E_{1g} mode always occurs below 200 cm^{-1}. In addition, a broad peak around 185 cm^{-1} in Fig. 2(a) corresponds to a two-phonon mode, which is always present in the VB group of TMDs.[39] In order to more clearly observe the exfoliated TaS_2 nanosheets in the experiment, a scanning electron microscope (SEM) was used to characterize the parameters such as the layer structure of the prepared TaS_2 nanosheets. An atomic force microscope (AFM) was used to observe the lateral size and thickness of the prepared materials. Figure 2(b) shows the SEM image. The lamellar structure of the nanosheets is clearly visible, and the successful exfoliation of the TaS_2 nanosheet material is confirmed.

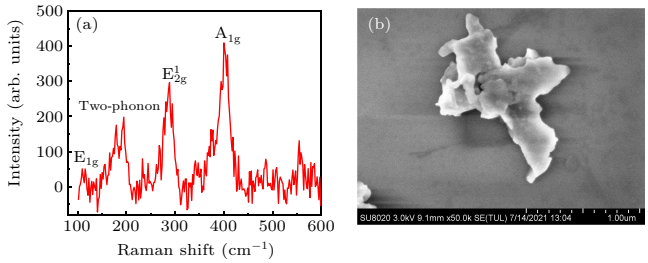


Fig. 2. (a) Raman spectrum of the prepared TaS_2 sample. (b) SEM image of TaS_2 nanosheets.

The AFM images are demonstrated in Fig. 3(a), and the thicknesses corresponding to the images are shown in Fig. 3(b). The thickness of TaS_2 nanosheets is between 15 nm and 20 nm, which confirms that the TaS_2 nanosheets contain fewer than 30 layers, as compared to the theoretical monolayer thickness of 0.66 nm. It is confirmed from the SEM and AFM images that the TaS_2 nanosheets are successfully stripped with transverse dimensions on the order of a few hundred nanometers.

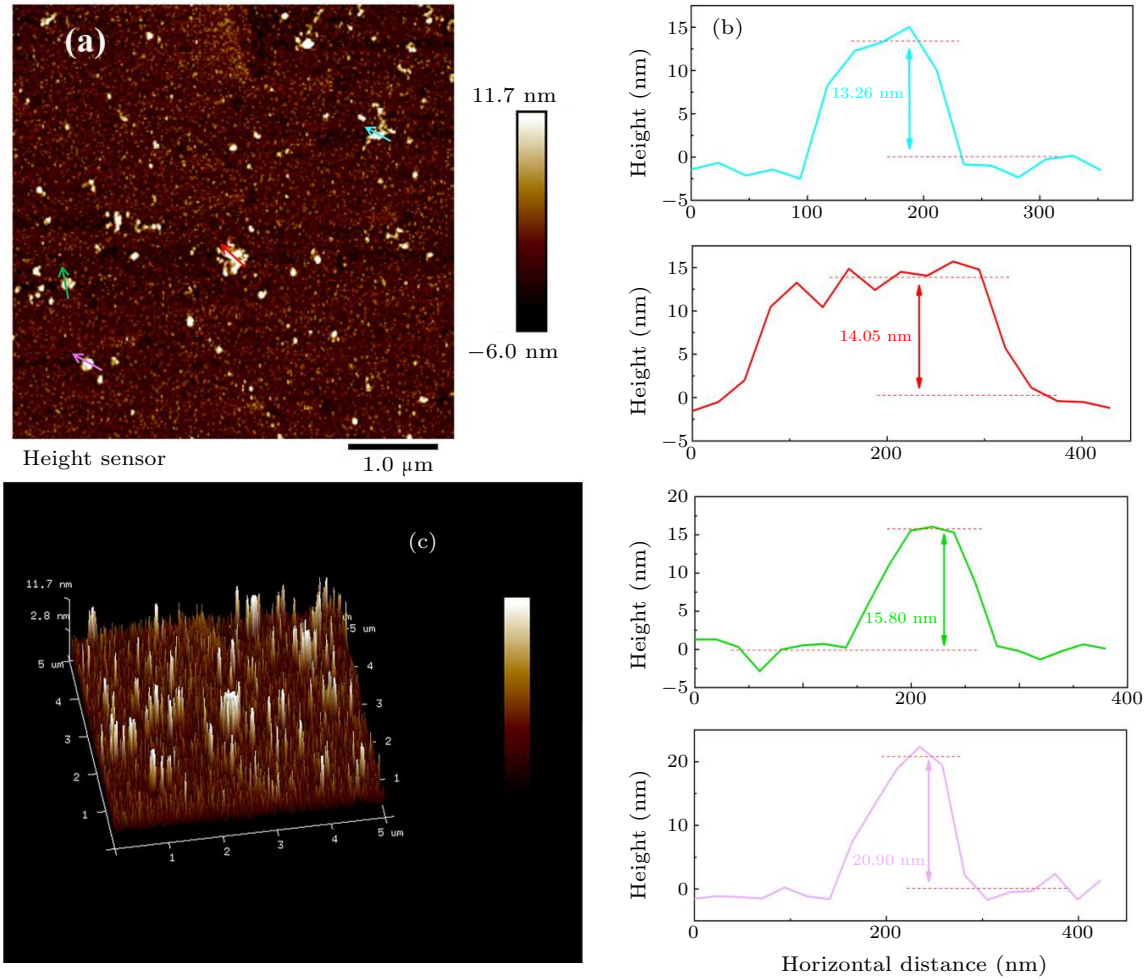


Fig. 3. (a) AFM image of TaS_2/PVA nanosheets. (b) The thickness of TaS_2 nanosheets. (c) Three-dimensional AFM image.

3. Experiment setup

Figure 4 depicts the experimental setup commonly used for the TaS_2 SA, which is employed in lasers with rare-earth-doped fiber. A 980 nm pump source is connected to the laser cavity to generate the pump laser. The polarization-independent tap-isolator-wavelength-division multiplexer (PI-TIWDM) is a compound device that consists of a wavelength division multiplexer, an optical coupler, and a polarization-independent isolator. Its implementation can notably facilitate laser construction. Ten percent of the laser portion is linked out of the annular cavity for experimental research. In this experiment, a 5-meter-long EDF is used for sufficient gain, with a dispersion parameter of -16 ps/(nm·km)$^{-1}$. The TaS_2-SA serves as a Q-switched component in the laser ring cavity. A polarization controller (PC) is inserted between the PI-TIWDM and TaS_2-SA, and the polarization state is adjusted by means of the PC. The fabricated TaS_2-based SA is employed to enhance the Q-switched parameters through the manipulation of the polarization state within the annular cavity. The remaining fibers and pigtails in the optical setup consist of single-mode fiber (SMF), with a dispersion parameter of ~ 17 ps/(nm·km)$^{-1}$. The total laser cavity length is 27.9 m. The output performance of the fiber laser is measured using a digital oscilloscope, a dynamometer, and a spectrum analyzer.

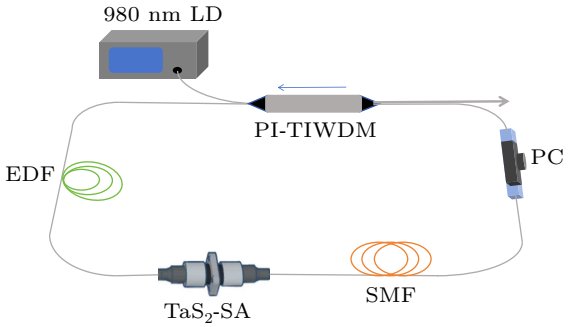


Fig. 4. Schematic diagram of the experimental setup.

4. Results and discussion

A continuous wave is observed on the oscilloscope during the experiment, which is powered by a pump source output of 8 mW. At 118 mW, the Q-switched images are found on an oscilloscope. In Fig. 5, the pump power is adjusted to 120 mW, 140 mW, 160 mW, 180 mW, 200 mW, 220 mW, and

230 mW in order to observe various pulse sequences. The schematic drawing indicates the absence of noticeable pulse modulation, manifesting that the *Q*-switched fiber laser is operating smoothly. When the pump power exceeds 180 mW, the *Q*-switched pulse amplitude decreases, which is caused by gain saturation. Once the peak power exceeds 231 mW, the *Q*-switched pulses vanish. The pump power has been restored to 231 mW, and the re-emergence of *Q*-switched phenomenon is observed. The pump power varies in the range from 118 mW to 231 mW, and *Q*-switched pulses are always present, indicating that the TaS_2/PVA is not damaged.

As shown in Fig. 6(a), we measure the output power and pulse energy as a function of pump power. The pump power varies in the range from 118 mW to 231 mW, corresponding to annular cavity output power linearly increasing from 528.9 μW to 1094 μW. Until the *Q*-switched image vanishes, the pulse energy can reach 13.1 nJ. The corresponding optical spectral characteristics of the TaS_2/PVA SA film are shown in Fig. 6(b). The center wavelength of the spectrum is located at 1560 nm with variation over a range of powers and with no change in width. The double *Y*-axis in Fig. 6(c) illustrates two linear trends, with the repetition rate gradually increasing from 51.33 kHz to 83.04 kHz as the pump power changes. Before the *Q*-switched image vanished, the pulse duration was reduced to 3.48 μs. We obtained a pulse full width at half maximum (FWHM) of 1.22 μs at 180 mW, as shown in Fig. 6(d). Under the pump power of 231 mW, the fiber laser operates for several hours and without any noticeable changes. Furthermore, despite adjustments to both the pump power and polarization state, no mode-locking operation is observed.

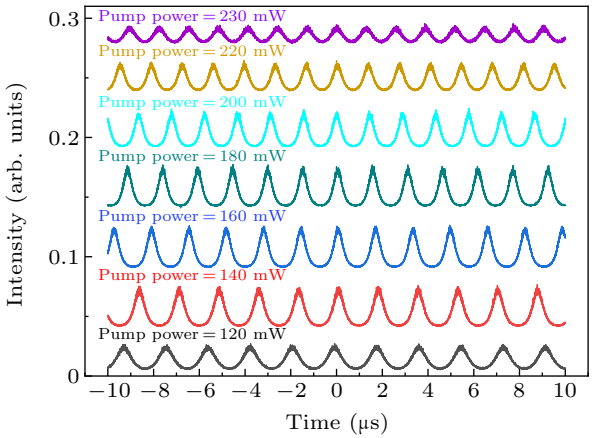


Fig. 5. The various pulse trains obtained under different pump powers.

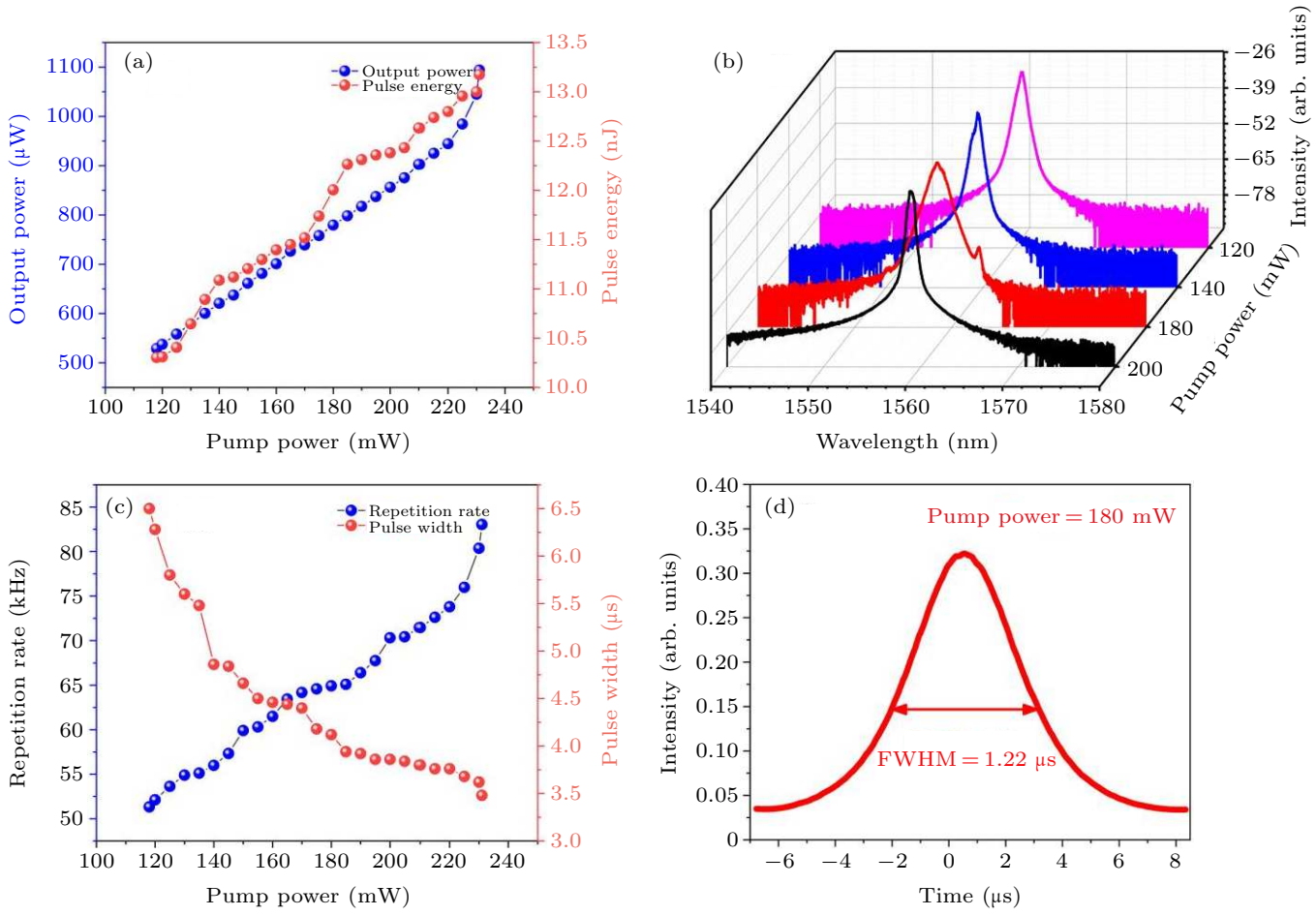


Fig. 6. (a) Output power and pulse energy versus incident pump power. (b) Optical spectra at pump powers of 120 mW, 140 mW, 180 mW, and 200 mW. (c) Pulse repetition rate and pulse duration as functions of pump power. (d) Single pulse profile.

Table 1. A comparison of passively Q-switched Er-doped fiber lasers based on different SAs.

SA	Center wavelength (nm)	Min pulse duration (μs)	Max pulse energy (nJ)	Max output power (mW)	Repetition rate (kHz)	Ref.
WSSe	1558.4	2.6	7.31	0.45	27.52–61.81	[40]
SWNTs	1555–1560	~ 7	14.1	~ 225 μW	~ 516	[41]
Bi_2Se_3	1565.14	13.4	13.4	~ 150 μW	4.508–12.88	[42]
$MoTe_2$	1557.8	1.4	4.6	0.4	44.4–77.8	[43]
P_3HT	1562	3.79	15.05	1.183	62.97–78.63	[44]
Graphene	1566.35	3.7	16.7	1.1	3.3–69.5	[45]
TaS_2	1560	3.48	13.1	1.094	51.33–83.04	this work

We attempt to verify whether the observed Q-switched operation originates exclusively from the saturable absorption properties of the TaS_2-based SA. For this reason, we removed the TaS_2 SA from the fiber laser. For the ring cavity without the TaS_2 SA, even if we kept varying the pump power or rotating the PC, we could not observe the Q-switched operation on the oscilloscope. The comparative results unequivocally demonstrate that the Q-switched operation is attributed to the saturable absorption of the SA based on the TaS_2. As shown in Table 1, TaS_2, as an SA, generates pulse output, featuring higher single-pulse energy and superior output power compared to nanomaterials such as $MoTe_2$ and WSSe.[40,41] Compared to other materials reported in earlier studies,[42–45] the output pulses have narrower pulse widths and higher repetition frequencies.

5. Conclusion

This work has exhibited the use of the TaS_2/PVA SA in the Q-switched EDF lasers. By inserting the TaS_2-SA film into the laser cavity, stable Q-switched pulses are achieved at a pump power of 118 mW. The passively Q-switched EDF laser operates at a central wavelength of 1560 nm. As the pump power increases from 118 mW to 231 mW, the repetition frequency correspondingly varies from 51.33 kHz to 83.04 kHz. At the maximum pump power of 231 mW, the single pulse energy reaches 13.1 nJ with a minimum pulse width of 3.48 μs. These experimental results prove that the TaS_2/PVA film is able to withstand the high power and possesses significant qualities suitable for applications in ultrafast photonics, rendering it an excellent candidate material for fiber laser applications.

Acknowledgments

Project supported by the National Natural Science Foundation of China (Grant No. 12075190) and the Shaanxi Fundamental Science Research Project for Mathematics and Physics (Grant No. 23JSY019).

References

[1] Lin H Y, Chuang Y J and Lin P J 2005 *Sci. Rep.* **11** 9525
[2] Vrijman C, Van Drooge A, Limpens J, Bos J, Van Der Veen J, Spuls P and Wolkerstorfer A J 2011 *Br. J. Dermatol.* **165** 934
[3] Tabata N, Yagi S and Hishii M J 1996 *Mater. Process. Technol.* **62** 309
[4] Chen X, Lotshaw W, Ortiz A, Staver P, Erikson C, McLaughlin M and Rockstroh T 1996 *J. Laser Appl.* **8** 233
[5] Jia X, Zhang Y, Chen Y, Wang H, Zhu G and Zhu X 2019 *Int. J. Adv. Manuf. Technol.* **104** 1269
[6] Puttnam B J, Rademacher G and Luís R S 2021 *Optica* **8** 1186
[7] Shen J P, Chen Y, Chen L, Xing F Y, Zhang F B, Xia R Z, Zuo H Y, Xiong F and Jiang R R 2025 *Chin. Phys. Lett.* **42** 044202
[8] Bruder F K, Hagen R, Rölle T, Weiser M S and Fäcke T 2011 *Angew. Chem. Int. Ed.* **50** 4552
[9] Partovi A, Peale D, Wuttig M, Murray C A, Zydzik G, Hopkins L, Baldwin K, Hobson W S, Wynn J and Lopata J 1999 *Appl. Phys. Lett.* **75** 1515
[10] Shen J, Xu S, Jiang R, Wang W, Zhang S, Xing F, Chen Y and Chen L 2024 *Chin. Phys. Lett.* **41** 034201
[11] Li H, Liu H, Yang Y, Lu R and Chen X 2022 *Chin. Phys. Lett.* **39** 034201
[12] Zhang M, Chi Z, Wang G, Fan Z, Wu H, Yang P, Yang J, Yan P and Sun Z 2022 *Adv. Mater.* **34** 2205679
[13] Drobczyński S and Duś-szachniewicz K 2016 *J. Opt. Soc. Am. B* **34** 38
[14] Chen X, Liu T, Zhang W, Guo D and Zhu H 2024 *Microw. Opt. Technol. Lett.* **66** e33880
[15] Guo B, Xiao Q L, Wang S H and Zhang H 2019 *Laser Photon. Rev.* **13** 1800327
[16] Sakata H, Takahashi N and Ushiro Y 2018 *Appl. Phys. B* **124** 1
[17] Shang Z, Wang G, Li J, Huang Q, Sun J, Cheng R, Zhang M, Yang J, Zhang Z and Yin J 2023 *Opt. Lett.* **48** 2768
[18] Yang H, Qi M, Li X, Xue Z, Cheng J, Lu C, Han D, Li L, Zhang Y and Zhao F 2023 *Opt. Express* **31** 38688
[19] Pang L, Jiang L, Zhao M, Zhang J, Zhao Q, Li L, Wu R, Lv Y and Liu W J 2025 *J. Mater. Sci. Technol.* **223** 208
[20] Li L, Pang L H, Wang R, Zhang X, Hui Z, Han D, Zhao F and Liu W J 2022 *Laser Photon. Rev.* **16** 2100255
[21] Li L, Cheng J W, Zhao Q Y, Zhang J N, Yang H, Zhang Y, Hui Z, Zhao F and Liu W J 2023 *Opt. Express* **31** 16872
[22] Wang G, Sheng Q, Tang S, Li Q, Xiong S, Lu C, Bai C, Zhang W, Zhang H and Fu S 2023 *Opt. Express* **31** 26145
[23] Shang X, Xu N, Guo J, Sun S, Zhang H, Wageh S, Al-Ghamdi A A, Zhang H and Li D 2023 *Sci. China Phys. Mech. Astron.* **66** 254211
[24] Li L, Lv R, Liu S, Wang X, Wang Y, Chen Z and Wang J 2018 *Laser Phys.* **28** 055106
[25] Mao D, Wang H Q, Zhang H Z, Zeng C, Du Y Q, He Z W, Sun Z P and Zhao J L 2021 *Nat. Commun.* **12** 6712
[26] Yang H R, Qi M T, Li X P, Xue Z, Lu C H, Cheng J W, Han D D and Li L 2024 *Chin. Phys. Lett.* **41** 014202
[27] Si Z Z, Dai C Q and Liu W J 2024 *Chin. Phys. Lett.* **41** 020502
[28] Li L, Xue Z, Pang L H, Xiao X S, Yang H R, Zhang J N, Zhang Y M, Zhao Q Y and Liu W J 2024 *Opt. Lett.* **49** 1293
[29] Xiao Y J, Xing X W, Cui W W, Chen Y Q, Zhou Q and Liu W J 2023 *Chin. Phys. Lett.* **40** 054201
[30] Wang H Y, Xiao Y J, Liu Q, Xing X W, Yang H J and Liu W J 2023 *Chin. Phys. Lett.* **40** 114204
[31] Meng X C, Li L, Sun N Z, Xue Z, Liu Q, Ye H and Liu W J 2023 *Chin. Phys. Lett.* **40** 124202
[32] Wang S, Yu H, Zhang H, Wang A, Zhao M, Chen Y, Mei L and Wang J 2014 *Adv. Mater.* **26** 3538
[33] Liu H, Luo A P, Wang F Z, Tang R, Liu M, Luo Z C, Xu W C, Zhao C J and Zhang H 2014 *Opt. Lett.* **39** 4591

[34] Chen X, Zhang Z, Ding Z, Liu J and Wang L 2016 *Angew. Chem.* **128** 10532
[35] Aguey-Zinsou F, Guo Z, Ng Y H and Wang D W 2018 *Chempluschem* **83** 890
[36] Wang H, Wang W, Zhong Y, Li D, Li Z, Xu X, Song X, Chen Y, Huang P and Mei A 2022 *Adv. Mater.* **34** 2206122
[37] Pang L, Li L, Liu W, Wu R and Lv Y 2020 *Opt. Mater.* **102** 109784
[38] Bendenia C, Merad-Dib H, Bendenia S and Hadri B 2018 *Optik* **174** 167
[39] Yang H, Li X, Han D, Zhao Q, Li L, Gong Y and Zhao F 2022 *Opt. Laser Technol.* **149** 107895
[40] Ahmad H, Tiu Z C and Ooi S I 2018 *Chin. Opt. Lett.* **16** 020009
[41] Zhou D P, Wei L, Dong B and Liu W K 2009 *IEEE Photon. Technol. Lett.* **22** 9
[42] Chen Y, Zhao C, Huang H, Chen S, Tang P, Wang Z, Lu S, Zhang H, Wen S and Tang D 2013 *J. Lightwave Technol.* **31** 2857
[43] Ahmad H, Azmy N F, Yusoff N, Reduan S A, Aidit S N, Bayang L and Samion M Z 2021 *Optik* **243** 167157
[44] Samsamnun F S, Zulkipli N F, Sarjidan M, Harun S W, Majid W, Khudus M I M A, Shuhaimi A, Rosol A H A, Rusdi M and Jafry A A A 2020 *Opt. Fiber Technol.* **54** 102073
[45] Luo Z, Zhou M, Weng J, Huang G, Xu H, Ye C and Cai Z 2010 *Opt. Lett.* **35** 3709